J. Min. Metall. Sect. B-Metall. 50 (1) B (2014) 87 - 90

Journal of Mining and Metallurgy, Section B: Metallurgy

Letter to Editor

INVESTIGATION OF DEFORMATION AND MICROSTRUCTURE OF BAINITE IN Cu-9.97%Al-4.62%Mn ALLOY

E. Aldirmaz [a, *], I. Aksoy [b]

[a] Department of Physics, Faculty of Science and Arts, Amasya University, Amasya, Turkey.
[b] Department of Physics, Faculty of Science and Arts, Kırıkkale University, Yahsihan Campus, Turkey.

(Received 04 July 2012; accepted 12 February 2014)

Abstract

In this study, some physical and mechanical properties in Cu-9.97%Al-4.62%Mn (wt%) alloy were investigated by X-ray diffraction (XRD), Scanning Electron Microscopy (SEM) and compression deformation test. Bainite phase were obtained in the samples according to SEM and XRD analyses. Compression stress was applied on the alloy in order to investigate the deformation effect on the bainite phase transformation. On the surface of the Cu-9.97%Al-4.62%Mn alloy after the deformation, both bainite and martensite variants formed.

Keywords: Bainite; Plastic Deformation; Scanning Electron Microscopy (SEM); X-ray Diffraction (XRD).

1. Introduction

Because of low price and high recovery force (only secondary to Ni–Ti alloy), Cu-based shape memory alloys have an extensive application field. However, the stabilization of martensite and decomposition of parent phase are problematic, which may degrade shape memory performance [1, 2]. According to the different heat treatments, quenching techniques, and chemical compositions, steels and other alloys can display different product phases such as bainite, pearlite, and martensite [3-7]. Since the discovery of bainitic transformation in 1920s, controversies on the true nature of this transformation, i.e. whether the transformation is diffusion-controlled or shear type deformation-controlled, have continued [8-13]. Bainite is the most complicated microstructure of steel. It is well known that two distinct forms of bainite, classified as upper and lower bainite, occur in steels in different temperature ranges [14]. The upper bainite forms at temperatures between 350°C and 550°C and is often characterized by a feathery structure. The lower bainite occurs at temperatures between 250°C and 350°C and is often characterized by a needle-like structure [15, 16]. Cu-based shape memory β-phase alloys exhibit order-disorder transformation at high temperatures. Although the β_1'-phase is metastable, it remains stable at room temperature upon quenching from the high temperature β-phase [17, 18]. Metastable parent β_1(B2 or DO_3) and martensitic β_1' (M9R or M18R) phases are transformed to bainitic α_1 (9R), complex cubic γ_2, or f.c.c. α phases by thermally activated processes [19]. In the majority of copper-based alloys, the bainite phase transformation has been found. Bainitic transformation occurs in these copper-based alloys, and β -phase forms diffusionally [20-22]. However, these phase transformations may result in a drastic drop in shape memory capacity and change of martensitic characteristic temperature [23].

The present study aimed to investigate the effect of deformation on microstructure of bainite transformation in Cu-9.97%Al-4.62%Mn alloy. Although there are many studies reporting some physical properties of bainite in Cu-9.97%Al-4.62%Mn alloy, literature reveals no studies on the effects of deformation on microstructure and mechanical properties of bainite transformations for the related composition of alloy.

2. Experimental

The composition of the alloy used in the present study was Cu-9.97%Al-4.62%Mn (wt%), which was prepared by vacuum induction melting under an argon atmosphere from pure (99.9 %) alloying elements. After this alloying, product alloy was cylindrical bars with 1 cm diameter and 10 cm length [22]. The samples were homogenized at 800 °C for 1 h and cooled to 25 °C furnace, and then air-cooled. This sample is denoted as A. Subsequently, homogenized specimens were compressed by 7 % plastic

* *Corresponding author: ealdirmaz@gmail.com*

DOI:10.2298/JMMB120704004A

deformation with an INSTRON 8510-type machine, operated at a constant strain rate of 0.2 mm/min at room temperature. Compression sample was prepared in the shape of rectangular pieces with 8×4×4 mm dimensions. This sample is denoted as B. The bulks A and B used in the SEM observations were mechanically polished and etched in a solution composed of 2.5 g $FeCl_3.6H_2O$ and 48 ml methanol in 10 ml HCl for 10 minutes. SEM observations were made using a JEOL 5600 scanning microscope, operated at 20 kV. X-ray diffraction patterns of the powder samples were taken by using a Bruker D8 Advance diffractometer. For these examinations, the monochromatic copper K_α radiation with wavelength of 1.5418 Å was used [22].

3. Results and discussion

3.1. SEM Observations

The undeformed and deformed samples were characterized by means of SEM and their microstructures were compared in Fig. 1(a) and (b), respectively. In SEM micrograph of the sample A, bainite transformation was formed. In addition, in some regions needle-like and rod-shaped and precipitates could be seen simultaneously (see Fig. 1(a)). Based on obvious morphological evidence, precipitates appear clearly and different in morphology; bainite structures have different orientations in different grains (Fig.1(a)) [24]. In sample A, the rod-shaped bainite disappeared after deformation. The plate-like bainite and γ_1' martensite structures formed in the same sample (see Fig.1(b)). In Cu-Al-Mn SMAs, it was seen that two types of martensite structures, 18R and 2H, formed depending on alloy composition, heat treatment and deformation. Martensites appear to be predominantly in the typical morphology of γ_1' martensite with effect of the deformation, these results are in agreement with the observation made by previous study [25]. It is known that the driving force necessary for the nucleation of the γ_1' martensite is larger than that of the β_1' martensite [26, 27]. In our study, the driving force occurred in sample B during the deformation is larger than that of sample A [28, 29]. Thus, it can be said that microstructure of the sample B is composed of γ_1'(2H) martensite variants with plate-like bainite [24, 30].

3.2. XRD Measurement

In order to determine the crystal structure of the Cu-Al-Mn alloy, the powder samples of the alloy were obtained. The phases of X-ray diffraction sample of Cu-Al-Mn alloy is determined by comparing the data obtained with those published in the literature [31]. By using these data, the unit cell parameters of the phases were calculated with POWD 2.2. computer program. Related peak positions of the phases were noted in the diffractogram of the samples A and B as shown in Fig. 2(a) and (b), on which diffraction peaks have been indexed.

XRD observations showed that phase transformation occurred in sample A and B. These phase was identified as α_1 bainite (9R), and the lattice parameters a = 0,452 nm b = 0,264 nm and c = 1,918 nm from the X-ray analyses were used [31]. Most of β-phase alloys are divide into two types according to the superlattices or composition ratio. One type is denoted by β_2-phase, which has a CsCl-type B2 superlattice and other type is denoted by β_1-phase, which has a Fe_3Al-type DO_3 superlattice [32]. Sample B was observed, γ_1'(2H) from DO_3 parent phase. This behavior can be explained in effects of the 7% deformation. The bainite may possess either M18R or M9R type ordered structure, depending on the type of order in the parent phase, as observed in Cu-Zn-Al alloys [33, 34]. In addition, X-ray diffraction of the sample B, as shown in Fig. 2(b), exhibited the peaks corresponding to γ_2 precipitates. In these alloys due to the formation of a large amount of aluminum rich particles of γ_2 precipitate, there was a decrease in the aluminum

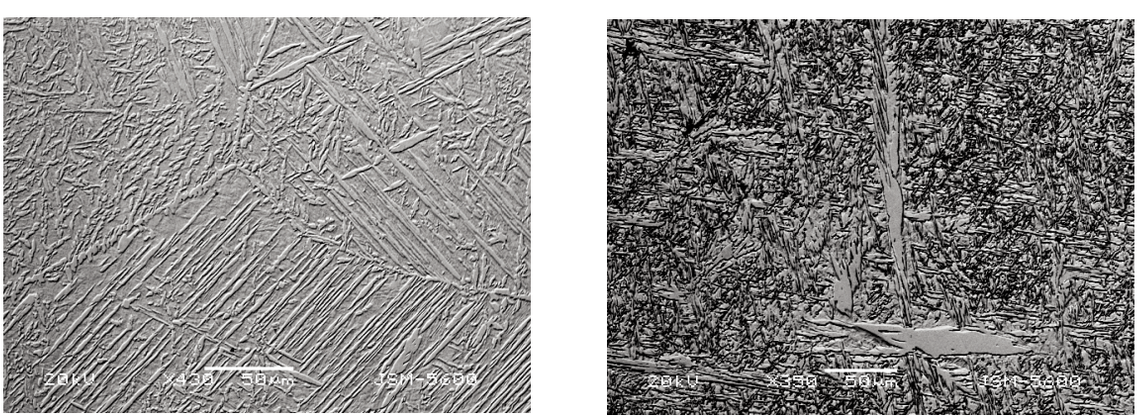

Figure 1. *Scanning electron micrographs of the bainite structures: (a) sample A (b) sample B.*

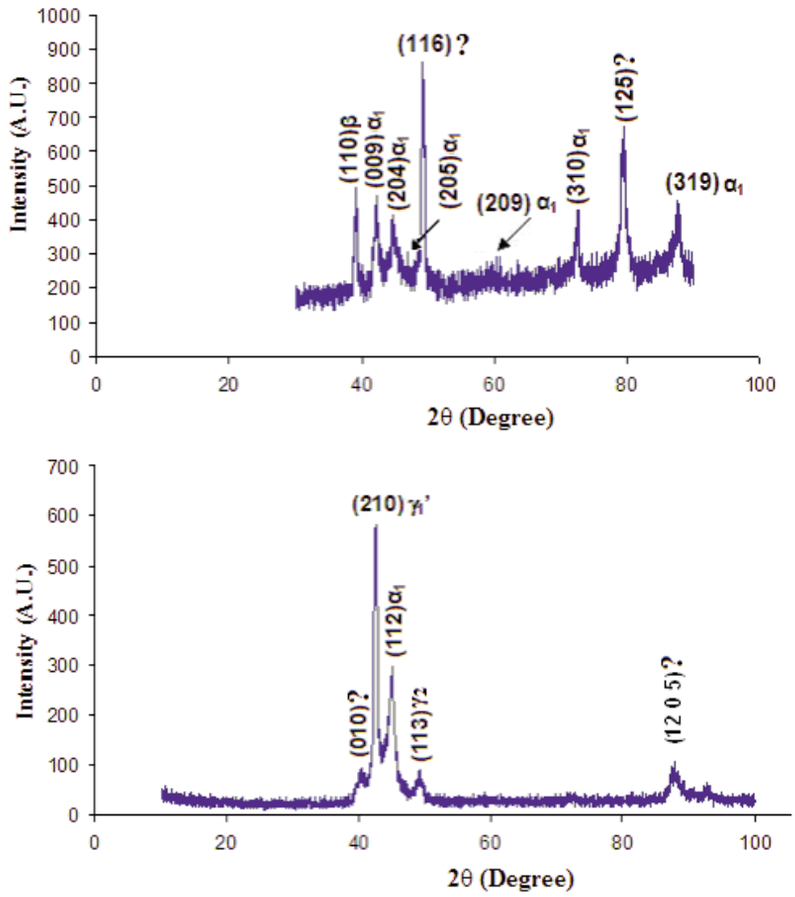

Figure 2. *X-ray diffraction patterns of samples (a) sample A and (b) sample B.*

concentration in the parent austenitic phase [35].

4. Conclusions

The results of this study can be summarized as follows: In the present study, bainite was formed over a wide range of temperatures, and the two types of bainite morphology in Cu-%9.97Al-%4.62Mn alloy were rod-shaped bainite and a needle-like bainite. The microstructure of the alloy was still composed of bainite phase with some precipitations after the thermal effects. In sample B with deformation, only a needle-like bainite and some martensite variants were formed.

References

[1] K.Sugimoto, K.Kamei, M.Nakaniwa, Engineering Aspects of Shape Memory Alloys, Edited by Duerig, Butterworth-Heinemann Ltd., 1990, pp:89-95.

[2] Y. Nakata, O. Yamamoto, K. Shimizu, Mater. Trans. JIM, 5 (1993) 429-437.

[3] S.A. Sajjadi, S.M. Zebarjad, J. Mater. Process. Technol., 189 (2007) 107-113.

[4] Z.G. Yang, H.S. Fang, Mater. Science., 9 (2005) 277-286.

[5] F.L.G. Oliveira, M.S. Andrade, A.B. Cota, Mater. Charact., 58 (2007) 256-261.

[6] A.M. Elwazri, P. Wanjara, S. Yue, Mater. Sci. Eng. A, 404 (2005) 91-98.

[7] J. Dash, H.M. Otte, Acta Metallurgica (1963) 1169-1178.

[8] E.S. Davenport, E.C. Bain, Trans. AIME, 90 (1930) 117-154.

[9] H.I. Aaronson, C. Laird, K.R. Kinsman, Metals Park, OH. (1970) 313-396.

[10] H.I. Aaronson, Metall London, (1979) 1.

[11] Y. Ohmori, Mater. Trans. JIM, 30 (1989) 487-497.

[12] J.M. Howe, Metall. Mater. Trans., 25A (19949 1917-1922.

[13] H.K.D.H. Bhadeshia, Bainite in Steels, second ed; Institute of Materials, London, 2001.

[14] H.I. Aaronson, C. Wells, Symposium on the Mechanism of Phase Transformations in Metals. Trans. AIME, Institute of Metals, London, 1955, pp. 47.

[15] A.K. Sinha, Ferrous Physical Metallurgy, Butterworth Publishers, London, 1989.

[16] W.F. Smith, Structure and Properties of Enginering Alloys, 2th ed., Mc-Graw-Hill,1994.

[17] M.A. Morris, Acta Materialia, 40 (1992) 1573-1586.

[18] A.G. Magdelena, A.T. Adorno, R.A.G. Silva, T.M. Carvalho, J Therm Anal Calorim., 97(1) (2009) 47–51.

[19] N.F. Kennon, D.P. Dunne, L. Middleton, Metall. Trans., 13A (1982) 551-555.

[20] K. Takesava, S. Sato, Mater. Trans. JIM, 32 (1991) 766-773.

[21] M.H. Wu, J. Perkins, C.M. Wayman, Acta Metal. Mater., 37 (1989) 1821-1837.

[22] E. Aldirmaz, H. Celik, I. Aksoy, Acta Physica Polonica A 124 (2013) 87-89.

[23] Z.Y. Pan, Z. Li, M.P. Wang, C.P. Deng, S.H. Li, F. Zheng, Mater. Sci. and Eng. A, 467 (2007) 104–107.

[24] Z.G. Wei, H.Y. Peng, W.H. Zou, D.Z. Yang, Metal. Mater. Trans. A, 28A (1997) 955-967.

[25] U. Sarı, T. Kırındı, Mater. Charac., 59 (2008) 920-929.

[26] H. Sakamoto, K. Shimizu, ISIJ Int., 29 (1989) 395–404.

[27] R. Kainuma, S. Takahashi, K. Ishida, Metall. Mater. Trans. A, 27A (8) (1996) 2187–2195.

[28] V. Recarte, R.B. Perez-Saez, E.H. Bocanegra, M.L. N´o, J. San Juan, Metall. Mater. Trans. A, 33A (2002) 2581–2591.

[29] J. Malimanek, N. Zarubova, Scr. Metal. Mater., 32 (1995) 1347–1352.

[30] H.K.D.H. Bhadeshia, Worked Examples in the Geometry of Crystals, London, 2001.

[31] Eon-Sik Lee, K. Young, Scripta Metal. Mater., 24 (1990) 745-750.

[32] S. Miyazaki, K. Otsuka, ISIJ Int., 29 (1989) 353–77.

[33] Y. Hamada, M.H. Wu, C.M. Wayman, Mater. Tran., JIM, 32 (1991) 747-756.

[34] M.H. Wu, Y. Hamada, C.M. Wayman, Metall. Mater. Trans. A, 25A (1994) 2581-2599.

[35] U.S. Mallik, V. Sampath, Mater. Sci. Eng. A, 478 (2008) 48–55.